Open access • Journal Article • DOI:10.2514/1.17857

Decentralized Coordinated Attitude Control Within a Formation of Spacecraft

Matthew C. VanDyke, Christopher Hall

Institutions: Virginia Tech

Published on: 01 Sep 2006 - Journal of Guidance Control and Dynamics (American Institute of Aeronautics and Astronautics, AIAA)

JOURNAL OF GUIDANCE, CONTROL, AND DYNAMICS
Vol. 29, No. 5, September–October 2006

Decentralized Coordinated Attitude Control Within a Formation of Spacecraft

Matthew C. VanDyke* and Christopher D. Hall†
Virginia Polytechnic Institute and State University, Blacksburg, Virginia 24061

DOI: 10.2514/1.17857

The problem of controlling the attitude of spacecraft within a formation is investigated. A class of decentralized coordinated attitude control laws using behavior-based control is developed. The decentralized coordinated attitude control laws that comprise the class differ by the coordination architecture used by the spacecraft formation. The choice of behavior weights defines the coordination architecture. A corollary of Barbalat's Lemma is used to prove that the class of control laws globally asymptotically stabilizes the spacecraft formation. Convergence of the system is shown to be a consequence of the closed-loop equations of motion. Numeric simulation is used to reinforce the analytic results, and to briefly investigate the effect of coordination architecture on performance.

Introduction

A spacecraft formation is a distributed system. A distributed system is a system consisting of multiple subsystems. The attitude control systems of individual spacecraft act as local control agents. The control decisions of the local control agents must be coordinated to ensure the stability and convergence of the global system.

Coordinated controllers are generally categorized into centralized and decentralized types. The distinction is based on where the control decisions are made. Centralized control is a type of coordinated control where a single control agent determines the control actions for the distributed system. In decentralized control, control decisions are relegated to the local control agents. The local control agents use local observations and any information communicated from the other control agents to determine control actions. Hybrid controllers using a combination of centralized and decentralized coordination are also possible.

The two primary benefits of decentralized control over centralized control are fault-tolerance and simpler control laws. Failure of a single local control agent in a decentralized controlled system does not necessarily lead to the destabilization of the entire system [1]. The failure is confined to the region of the failed local control agent resulting in a graceful degradation of system performance. Decentralized control results in relatively simple control laws, because the design of the global controller can be decomposed into smaller control agents. The local control agents are designed so that they perform their local control tasks, and coordinate with one another to control the global system [1]. The coordination is implemented by means of communication between the local control agents. Centralized controllers require greater information and information processing than what is required by the local control agents of the equivalent decentralized controller [2]. The primary drawback of decentralized controllers is that they are difficult to analyze analytically.

A useful tool for the coordinated attitude control problem is behavior-based control. Behavior-based control is implemented when a control system has multiple, and sometimes competing, objectives or behaviors. The behaviors could include goal-attainment, collision-avoidance, obstacle-avoidance, and formation-keeping. The overall control action is determined by a weighted sum of the control actions for each of the behaviors [3].

For the coordinated attitude control problem, behavior-based control is used to arrive at a compromise between the control actions required for the formation-keeping and station-keeping behaviors [4]. Station-keeping is the behavior that tries to drive the spacecraft to its absolute desired attitude. Formation-keeping is the behavior that tries to align the spacecraft with the other spacecraft in the formation. The behavior-based attitude control of a spacecraft that is within a formation drives the spacecraft to an attitude that is a compromise between its absolute desired attitude and the attitudes of the other spacecraft in the formation.

Both centralized and decentralized coordination approaches to the coordinated attitude control problem have been analyzed. The centralized coordination approaches have been examined in detail [5–13]; however, there are still gaps in the decentralized coordinated attitude control literature [4,14–17]. The most notable gap is the lack of a decentralized coordinated attitude controller that guarantees global convergence of the spacecraft formation. The research presented here extends the previous work in decentralized coordinated attitude control. A class of decentralized coordinated attitude control laws that guarantees global convergence of the spacecraft formation is developed and analyzed.

Literature Review

The coordinated spacecraft control area has been studied primarily by three schools. The first school investigates leader–follower type coordination strategies. The papers of the second school concentrate on behavior-based and virtual structure coordination strategies. The third school uses a fundamentally different approach than the first two schools, where the control law and the coordination layer are decoupled.

An early coordinated attitude control paper from the first school is by Wang and Hadaegh [5]. In their paper a nearest-neighbor attitude controller is developed and proven to globally asymptotically stabilize the attitude of the spacecraft formation. The nearest-neighbor controller uses a leader–follower coordination architecture with multiple leaders. The nearest-neighbor attitude controller uses a "chain" coordination architecture, where each spacecraft follows one other spacecraft in the formation, except the leader who tracks the absolute desired attitude trajectory of the formation. In a subsequent paper, Wang et al. [6] use the same type of formulation to develop one-leader based coordinated control laws for position and attitude control within a spacecraft formation.

The second school of researchers uses an approach that is similar to the first school; however, they investigate more exotic methods of

Received 23 June 2005; revision received 3 February 2006; accepted for publication 4 February 2006.

*Formerly Graduate Research Assistant, Aerospace and Ocean Engineering Department. Currently Attitude Control Systems Engineer, Orbital Sciences Corporation, Dulles, Virginia. Member AIAA.

†Professor, Aerospace and Ocean Engineering Department. Associate Fellow AIAA.

coordinated control. Lawton et al. [14] develop a decentralized controller for the coordinated attitude control problem that they term the coupled dynamics controller. The coupled dynamics controller uses a ring communication topology, where each spacecraft knows the state of two other spacecraft in the formation. The desired state and the state of the two other spacecraft are used to determine the appropriate control torque. A convergence proof is provided; however, the proof does not ensure global convergence of the formation attitude. It requires that the spacecraft begin with no angular rate and that the initial formation error is below a certain limit. In another paper, Lawton and Beard [17] develop a passivity-based controller for the coordinated attitude control problem. The passivity-based controller uses only attitude information to determine control actions, thus alleviating the need for angular rate measurements. The authors analytically determine the domain of attraction for the passivity-based controller and the coupled dynamics controller. The coupled dynamics and passivity-based controllers use behavior-based control. A more general architecture for spacecraft formation attitude control is introduced by the same authors in a later paper [4]. The architecture is designed to subsume the leader–follower, behavior-based, and virtual-structure coordination strategies. Ren and Beard [13] investigate a centralized implementation of virtual structure coordination strategy using the general architecture. The primary contribution of the paper is the addition of formation feedback to the spacecraft formation. The authors prove the virtual structure control law guarantees the stability and convergence of the system.

The approach to the design of coordinated controllers by the third school is different from the approaches used by the first two schools. The third school decouples the individual attitude controllers from the coordinated controller. The goal of the third school is slightly different. The first two schools strive to guarantee convergence of the formation, whereas the third school looks to stabilize the formation to a final state that minimizes the relative and absolute errors of the spacecraft in the presence of tracking errors. A coordinated controller based on decentralized feedback is introduced by Kang et al. [11]. A reference projection is used to determine the appropriate control action for the spacecraft. Each spacecraft in the formation uses its current desired state and state information communicated by the other spacecraft to determine a quasi-desired state using the reference projection. The quasi-desired state is then used by the spacecraft's attitude controller to determine the appropriate control action. Different types of coordination are possible using the appropriate reference projection. In a later paper, Kang and Yeh [9] first discuss applying the idea of reference projections to tracking control. Kang and Sparks [12] investigate the idea further and present simulation results.

The literature on coordinated attitude control uses some interesting and novel methods to attack the coordinated control problem, such as behavior-based control and reference projections. However, the literature suffers from two deficiencies. The first is the poor definition of kinematic error variables used in the development of the coordinated controllers, and the second is the lack of global stability and convergence proofs for the decentralized coordinated controllers. The kinematic attitude error quantities used by the authors of the first and third school are differences between quaternions or angular velocity vectors, in different reference frames. These error measures are not globally physically significant quantities. Despite the use of poorly defined error measures, valid analytic proofs are provided by all three schools. Authors from the first and second schools offer global stability and convergence proofs for centralized leader–follower type coordinated controllers. Local analytic stability and convergence proofs are offered by authors from the second school for their decentralized coupled dynamics controller. The third school also offers a local stability proof for its reference projection based coordinated attitude controllers. However, analytic proofs of global convergence for decentralized coordinated controllers do not appear in the literature.

The deficiencies of the literature noted here are addressed and resolved by this work. Globally significant kinematic error variables are defined and used in the development of a class of decentralized attitude control laws that guarantee global asymptotic stability of the attitude of spacecraft within a formation.

Table 1 Reference frame notation

Subscript	Description
i	Inertial reference frame
b	Body-fixed reference frame
$j, k = 0$	Desired spacecraft formation reference frame
$j, k = 1, 2, \cdots, n$	Body-fixed reference frame of spacecraft $1, 2, \cdots, n$

Spacecraft Attitude Dynamics

A brief review of spacecraft attitude dynamics is provided primarily to introduce notation. The quaternion, $\bar{\mathbf{q}}$, is defined as

$$\bar{\mathbf{q}} = \begin{bmatrix} \mathbf{e} \sin\left(\frac{\Phi}{2}\right) \\ \cos\left(\frac{\Phi}{2}\right) \end{bmatrix} = \begin{bmatrix} \mathbf{q} \\ q_4 \end{bmatrix} \tag{1}$$

where $\mathbf{e}$ is the Euler axis, Φ is the Euler angle, $\mathbf{q}$ is the vector part of the quaternion, and q_4 is the scalar part of the quaternion.[‡] The "canonical" quaternion, $\bar{\mathbf{p}}$, is defined

$$\bar{\mathbf{p}} = \text{sgn}(q_4)\bar{\mathbf{q}} = \begin{bmatrix} \mathbf{p} \\ p_4 \end{bmatrix} \tag{2}$$

where $\mathbf{p}$ is the vector part of the canonical quaternion, p_4 is the scalar part of the canonical quaternion, and the function $\text{sgn}(x)$ is defined

$$\text{sgn}\,(x) = \begin{cases} 1 & \text{if } x \geq 0 \\ -1 & \text{if } x < 0 \end{cases} \tag{3}$$

Use of the canonical quaternion is required to resolve the ambiguity in the quaternion representation that allows $\bar{\mathbf{q}}$ and $-\bar{\mathbf{q}}$ to represent the same rotation. The inverse canonical quaternion is defined

$$\bar{\mathbf{p}}^{-1} = \begin{bmatrix} -\mathbf{p}^{\mathsf{T}} & p_4 \end{bmatrix}^{\mathsf{T}} \tag{4}$$

which represents the equal and opposite rotation represented by $\bar{\mathbf{p}}$.

Subscripts are used to clarify the rotation represented by the quaternion and canonical quaternion. For example, $\bar{\mathbf{p}}_{jk}$ represents the rotation from reference frame k, $\mathcal{F}_k$, to reference frame j, $\mathcal{F}_j$. The subscripts used in this work are defined in Table 1. $\mathcal{F}_i$ is an inertially fixed reference frame. $\mathcal{F}_b$ is a body-fixed reference frame centered at the spacecraft's mass center. $\mathcal{F}_0$ defines the desired orientation of the spacecraft formation.[§] $\mathcal{F}_1$ through $\mathcal{F}_n$ are the body-fixed reference frames of spacecraft 1 through n.

The quaternion that represents the successive rotations of $\bar{\mathbf{p}}_{bc}$ and $\bar{\mathbf{p}}_{ab}$ is

$$\bar{\mathbf{q}}_{ac} = \bar{\mathbf{p}}_{ab} \otimes \bar{\mathbf{p}}_{bc} \tag{5}$$

$$\bar{\mathbf{q}}_{ac} = \begin{bmatrix} p_{4,ab} & p_{3,ab} & -p_{2,ab} & p_{1,ab} \\ -p_{3,ab} & p_{4,ab} & p_{1,ab} & p_{2,ab} \\ p_{2,ab} & -p_{1,ab} & p_{4,ab} & p_{3,ab} \\ -p_{1,ab} & -p_{2,ab} & -p_{3,ab} & p_{4,ab} \end{bmatrix} \begin{bmatrix} p_{1,bc} \\ p_{2,bc} \\ p_{3,bc} \\ p_{4,bc} \end{bmatrix} \tag{6}$$

The first time derivative of the quaternion is defined as

$$\dot{\bar{\mathbf{q}}}_{jk} = \frac{1}{2}\bar{\omega}_{jk} \otimes \bar{\mathbf{q}}_{jk} \tag{7}$$

where $\bar{\omega}_{jk}$ is defined

$$\bar{\omega}_{jk} = \begin{bmatrix} \omega_{jk}^{\mathsf{T}} & 0 \end{bmatrix}^{\mathsf{T}} \tag{8}$$

[‡]The notation x_n represents the nth component of the vector $\mathbf{x}$.

[§]$\mathcal{F}_0$ does not define the desired orientation of the individual spacecraft if a constant, nonzero attitude offset is desired.

and ω_{jk} is the angular velocity of $\mathcal{F}_j$ with respect to $\mathcal{F}_k$ expressed in $\mathcal{F}_j$.

The individual spacecraft in the formation are modeled as rigid bodies. The equations of motion for a rigid body are

$$\mathbf{I}_b\dot{\omega}_{bi} = \mathbf{g}_b - \omega_{bi}^{\times}\mathbf{I}_b\omega_{bi} \tag{9}$$

where $\mathbf{I}_b$ is the moment of inertia matrix of the spacecraft expressed in $\mathcal{F}_b$ and $\mathbf{g}_b$ is the external torque expressed in $\mathcal{F}_b$.

Attitude State Error

There are two measures of the attitude state[‖] error of a spacecraft within a formation. The error measures are the station-keeping and formation-keeping attitude state errors. Station-keeping error is the attitude state error of an individual spacecraft with respect to its absolute desired attitude state. The station-keeping attitude error for the jth spacecraft, $\bar{\mathbf{p}}_{j0}$, is defined

$$\bar{\mathbf{p}}_{j0} = \mathrm{sgn}(q_{4,j0})\bar{\mathbf{p}}_{ji} \otimes \bar{\mathbf{p}}_{0i}^{-1} \tag{10}$$

where $\bar{\mathbf{p}}_{0i}$ is the desired attitude of the spacecraft formation. The station-keeping angular velocity error, ω_{j0}, is defined

$$\omega_{j0} = \omega_{ji} - \mathbf{R}^{j0}\omega_{0i} \tag{11}$$

where ω_{0i} is the angular velocity of $\mathcal{F}_0$ with respect to $\mathcal{F}_i$ expressed in $\mathcal{F}_0$ and $\mathbf{R}^{j0}$ is the transformation matrix from $\mathcal{F}_0$ to $\mathcal{F}_j$.

Formation-keeping error is the attitude state error of an individual spacecraft with respect to the other spacecraft in the formation. The desired relative attitudes of the spacecraft in the formation are assumed to be constant. The equations developed in this section deal with the error between two spacecraft in the formation. The attitude error between the jth and kth spacecraft, $\bar{\mathbf{p}}_{jk}$, is

$$\bar{\mathbf{p}}_{jk} = \mathrm{sgn}(q_{4,jk})\bar{\mathbf{p}}_{j0} \otimes \bar{\mathbf{p}}_{k0}^{-1} \tag{12}$$

where

$$\bar{\mathbf{q}}_{jk} = \bar{\mathbf{p}}_{j0} \otimes \bar{\mathbf{p}}_{k0}^{-1} \tag{13}$$

The relative angular velocity vector of the jth spacecraft with respect to the kth spacecraft, ω_{jk}, is defined as

$$\omega_{jk} = \omega_{j0} - \mathbf{R}^{jk}\omega_{k0} \tag{14}$$

The equations relating the relative attitude states of the jth and kth spacecraft are

$$\omega_{kj} = -\mathbf{R}^{kj}\omega_{jk} \tag{15}$$

$$\mathbf{p}_{kj} = -\mathbf{p}_{jk} = -\mathbf{R}^{kj}\mathbf{p}_{jk} \tag{16}$$

Coordinated Attitude Control

The two desired behaviors of the attitude control system for a spacecraft within a formation are station-keeping and formation-keeping. The control action for the station-keeping behavior for the jth spacecraft, $\mathbf{g}_j^s$, is defined

$$\mathbf{g}_j^s = \omega_{ji}^{\times}\mathbf{I}_j\omega_{ji} + \mathbf{I}_j\mathbf{R}^{j0}\dot{\omega}_{0i} - \rho_{j0}^p\mathbf{p}_{j0} - \rho_{j0}^d\omega_{j0} \tag{17}$$

where ρ_{j0}^p and ρ_{j0}^d are the proportional and derivative station-keeping behavior weights. Equation (17) is an attitude trajectory tracking control law for a single spacecraft, and is similar to the control laws developed in Hall et al. [18]. If the desired attitude of the formation is constant, then the station-keeping control action can be simplified by not including the first two terms.

[‖]The term "attitude state" refers to both the attitude and angular velocity of a rigid body.

The control action for the formation-keeping behavior for the jth spacecraft, $\mathbf{g}_j^f$, is defined

$$\mathbf{g}_j^f = -\sum_{k=1}^{n}\rho_{jk}^p\mathbf{p}_{jk} - \sum_{k=1}^{n}\rho_{jk}^d\omega_{jk} \tag{18}$$

where ρ_{jk}^p is the proportional formation-keeping behavior weight, ρ_{jk}^d is the derivative formation-keeping behavior weight, and n is the number of spacecraft in the formation. The control action for the formation-keeping behavior drives the relative attitude state error, $\mathbf{p}_{jk}$ and ω_{jk}, between connected spacecraft to zero. The proportional behavior weighting factor, ρ_{jk}^p, determines the importance of the relative alignment of the jth and the kth spacecraft in the formation. The derivative behavior weight, ρ_{jk}^d, determines the importance of the jth and the kth spacecraft in the formation maintaining the same angular rate. Equation (18) is a generalization and refinement of the formation-keeping control action used by the velocity feedback controller presented in Lawton and Beard [17] and the "coupled-dynamics controller" presented in Lawton et al. [14].

The decentralized attitude control law is determined by summing the control actions for the station-keeping and formation-keeping behaviors. The resulting control law for the jth spacecraft, $\mathbf{g}_j$, is

$$\mathbf{g}_j = \mathbf{g}_j^s + \mathbf{g}_j^f = \omega_{ji}^{\times}\mathbf{I}_j\omega_{ji} + \mathbf{I}_j\mathbf{R}^{j0}\dot{\omega}_{0i} - \sum_{k=0}^{n}\rho_{jk}^p\mathbf{p}_{jk} - \sum_{k=0}^{n}\rho_{jk}^d\omega_{jk} \tag{19}$$

The use of the canonical quaternion in Eq. (19) results in a discontinuous control law.[¶] The behavior weights are restricted so that

$$\begin{array}{ll} \rho_{jk}^p = \rho_{kj}^p & \rho_{jk}^d = \rho_{kj}^d \\ \rho_{jk}^p \geq 0 & \rho_{jk}^d \geq 0 \quad \text{for } j,k = 1,2,\cdots,n \\ \rho_{j0}^p > 0 & \rho_{j0}^d > 0 \end{array} \tag{20}$$

$$\rho_{j0}^p > 2\sum_{k=1}^{n}\rho_{jk}^p \quad \text{for } j = 1,2,\cdots,n \tag{21}$$

Equation (20) lists the restrictions on the station-keeping and formation-keeping behavior weights to guarantee global asymptotic stability of the system. Equation (21) is a sufficient condition to guarantee convergence of the spacecraft formation's attitude.

Several assumptions are made to simplify the development and analysis of the class of decentralized attitude control laws. The desired relative attitudes of the spacecraft in the formation are constant. The desired attitude trajectory, $\bar{\mathbf{p}}_0$ and ω_0, of the spacecraft formation is bounded. The spacecraft are rigid bodies that use external torque actuation for attitude control.[**] Each spacecraft (j) has perfect knowledge of its own attitude state and the attitude states of the other spacecraft (k) in the formation for which there is a nonzero formation-keeping behavior weight ($\rho_{jk}^p \neq 0$ or $\rho_{jk}^d \neq 0$).

Global Asymptotic Stability Proof

The class of decentralized attitude control laws is proven to globally asymptotically stabilize the attitude of the spacecraft within the formation using a corollary of Barbalat's Lemma. The corollary states,

Corollary 1 [20] If a scalar function $V(\mathbf{x}, t)$ satisfies the following conditions:

1) $V(\mathbf{x}, t)$ is lower bounded
2) $\dot{V}(\mathbf{x}, t)$ is negative semidefinite
3) $\dot{V}(\mathbf{x}, t)$ is uniformly continuous in time

[¶]Because the control law is discontinuous, the theorem presented in Bhat and Bernstein [19] is not applicable.

[**]Although external torque actuation is used in developing the coordinated control laws, extending the results for internal torque actuation is a straightforward matter. The internal torque actuation extension is not included because there are no important nor significant differences in that development.

Then $\dot{V}(\mathbf{x}, t) \to 0$ as $t \to \infty$.

For this analysis, the scalar function V is defined

$$V = \sum_{j=1}^{n} V_j \tag{22}$$

where V_j is

$$V_j = \frac{1}{2}\omega_{j0}^{\mathsf{T}}\mathbf{I}_j\omega_{j0} + \rho_{j0}^{p}S_{j0} + \frac{1}{2}\sum_{k=1}^{n}\rho_{jk}^{p}S_{jk} \tag{23}$$

The function S_{jk} is defined

$$S_{jk} = \begin{cases} \mathbf{q}_{jk}^{\mathsf{T}}\mathbf{q}_{jk} + \rho_{jk}^{p}(1 - q_{4,jk})^2 & \text{if } q_{4,jk} \geq 0 \\ \mathbf{q}_{jk}^{\mathsf{T}}\mathbf{q}_{jk} + \rho_{jk}^{p}(1 + q_{4,jk})^2 & \text{if } q_{4,jk} < 0 \end{cases} \tag{24}$$

The function V is positive definite (and therefore lower bounded) and radially unbounded. The derivative of V is

$$\dot{V} = \sum_{j=1}^{n} \dot{V}_j \tag{25}$$

The derivative of V_j is

$$\dot{V}_j = \omega_{j0}^{\mathsf{T}}\mathbf{I}_j\dot{\omega}_{j0} + \rho_{j0}^{p}\dot{S}_{jk} + \frac{1}{2}\sum_{k=1}^{n}\rho_{jk}^{p}\dot{S}_{jk} \tag{26}$$

where the first time derivative of S_{jk} is

$$\dot{S}_{jk} = \begin{cases} \omega_{jk}^{\mathsf{T}}\mathbf{q}_{jk} & \text{if } q_{4,jk} \geq 0 \\ -\omega_{jk}^{\mathsf{T}}\mathbf{q}_{jk} & \text{if } q_{4,jk} < 0 \end{cases} = \omega_{jk}^{\mathsf{T}}\mathbf{p}_{jk} \tag{27}$$

Applying this to Eq. (26) results in

$$\dot{V}_j = \omega_{j0}^{\mathsf{T}}\mathbf{I}_j\dot{\omega}_{j0} + \rho_{j0}\omega_{j0}^{\mathsf{T}}\mathbf{p}_{j0} + \frac{1}{2}\sum_{k=1}^{n}\rho_{jk}^{p}\omega_{jk}^{\mathsf{T}}\mathbf{p}_{jk} \tag{28}$$

$$= \omega_{j0}^{\mathsf{T}}(\mathbf{I}_j\dot{\omega}_{j0} + \rho_{j0}^{p}\mathbf{p}_{j0}) + \frac{1}{2}\sum_{k=1}^{n}\rho_{jk}^{p}\omega_{jk}^{\mathsf{T}}\mathbf{p}_{jk} \tag{29}$$

The closed-loop attitude dynamics of the jth spacecraft, Eqs. (9) and (19), are used with Eq. (29) to arrive at

$$\dot{V}_j = -\omega_{j0}^{\mathsf{T}}\sum_{k=0}^{n}\rho_{jk}^{d}\omega_{jk} - \omega_{j0}^{\mathsf{T}}\sum_{k=1}^{n}\rho_{jk}^{p}\mathbf{p}_{jk} + \frac{1}{2}\sum_{k=1}^{n}\rho_{jk}^{p}\omega_{jk}^{\mathsf{T}}\mathbf{p}_{jk} \tag{30}$$

The first time derivative of V is

$$\dot{V} = -\sum_{j=1}^{n}\rho_{j0}^{d}\omega_{j0}^{\mathsf{T}}\omega_{j0} + \sum_{j=1}^{n}\left(-\omega_{j0}^{\mathsf{T}}\sum_{k=1}^{n}\rho_{jk}^{d}\omega_{jk} - \omega_{j0}^{\mathsf{T}}\sum_{k=1}^{n}\rho_{jk}^{p}\mathbf{p}_{jk} + \frac{1}{2}\sum_{k=1}^{n}\rho_{jk}^{p}\omega_{jk}^{\mathsf{T}}\mathbf{p}_{jk}\right) \tag{31}$$

Summing the terms involving the relative attitude variables of the lth and mth spacecraft results in

$$\sum_{j=l,m}\left(-\omega_{j0}^{\mathsf{T}}\sum_{k=l,m}\rho_{jk}^{d}\omega_{jk} - \omega_{j0}^{\mathsf{T}}\sum_{k=l,m}\rho_{jk}^{p}\mathbf{p}_{jk} + \frac{1}{2}\sum_{k=l,m}\rho_{jk}^{p}\omega_{jk}^{\mathsf{T}}\mathbf{p}_{jk}\right) = -\rho_{lm}^{d}\omega_{l0}^{\mathsf{T}}\omega_{lm} - \rho_{ml}^{d}\omega_{m0}^{\mathsf{T}}\omega_{ml} - \rho_{lm}^{p}\omega_{l0}^{\mathsf{T}}\mathbf{p}_{lm} - \rho_{ml}^{p}\omega_{m0}^{\mathsf{T}}\mathbf{p}_{ml} + \frac{1}{2}\rho_{lm}^{p}\omega_{lm}^{\mathsf{T}}\mathbf{p}_{lm} + \frac{1}{2}\rho_{ml}^{p}\omega_{ml}^{\mathsf{T}}\mathbf{p}_{ml} \tag{32}$$

Recognizing that the relative attitude variables are related simplifies the terms to

$$\sum_{j=l,m}\left(-\omega_{j0}^{\mathsf{T}}\sum_{k=l,m}\rho_{jk}^{d}\omega_{jk} - \omega_{j0}^{\mathsf{T}}\sum_{k=l,m}\rho_{jk}^{p}\mathbf{p}_{jk} + \frac{1}{2}\sum_{k=l,m}\rho_{jk}^{p}\omega_{jk}^{\mathsf{T}}\mathbf{p}_{jk}\right) = -\rho_{lm}^{d}(\omega_{l0} - \mathbf{R}^{lm}\omega_{m0})^{\mathsf{T}}\omega_{lm} - \rho_{lm}^{p}(\omega_{l0} - \mathbf{R}^{lm}\omega_{m0})^{\mathsf{T}}\mathbf{p}_{lm} + \rho_{lm}^{p}\omega_{lm}^{\mathsf{T}}\mathbf{p}_{lm} \tag{33}$$

The definition of the relative angular velocity vector, Eq. (14), is used to further simplify to

$$\sum_{j=l,m}\left(-\omega_{j0}^{\mathsf{T}}\sum_{k=l,m}\rho_{jk}^{d}\omega_{jk} - \omega_{j0}^{\mathsf{T}}\sum_{k=l,m}\rho_{jk}^{p}\mathbf{p}_{jk} + \frac{1}{2}\sum_{k=l,m}\rho_{jk}^{p}\omega_{jk}^{\mathsf{T}}\mathbf{p}_{jk}\right) = -\rho_{lm}^{d}\omega_{lm}^{\mathsf{T}}\omega_{lm} \tag{34}$$

which is a negative definite quantity. If this process is performed for each possible spacecraft pairing, $\dot{V}$ simplifies to

$$\dot{V} = -\sum_{j=0}^{n}\sum_{k=j+1}^{n}\rho_{jk}^{d}\omega_{jk}^{\mathsf{T}}\omega_{jk} \tag{35}$$

which is negative semidefinite.

The derivative of the scalar function is proven to be uniformly continuous in time by showing that the second time derivative of V is bounded. The second time derivative of V is

$$\ddot{V} = -2\sum_{j=0}^{n}\sum_{k=j+1}^{n}\rho_{jk}^{d}\omega_{jk}^{\mathsf{T}}\dot{\omega}_{jk} \tag{36}$$

Equation (35) requires $V(t) \leq V(0)$, which implies $\mathbf{q}_{jk}$, $\mathbf{p}_{jk}$, and ω_{jk} are bounded. Therefore, $\ddot{V}$ is bounded if $\dot{\omega}_{jk}$ is bounded. The first time derivative of ω_{jk} is

$$\dot{\omega}_{jk} = \dot{\omega}_{ji} - \mathbf{R}^{jk}\dot{\omega}_{ki} \tag{37}$$

and the first time derivative of ω_{ji} is

$$\dot{\omega}_{ji} = \mathbf{R}^{j0}\dot{\omega}_{0i} - \sum_{k=0}^{n}\rho_{jk}^{p}\mathbf{p}_{jk} - \sum_{k=0}^{n}\rho_{jk}^{d}\omega_{jk} \tag{38}$$

The desired attitude state of the spacecraft formation is bounded, $\ddot{V}$ is bounded, and $\dot{V}$ is uniformly continuous in time. The requirements of the corollary are satisfied, and

$$\lim_{t\to\infty}\omega_{jk} = \mathbf{0} \quad \text{for } j = 1, 2, \cdots, n \quad \text{and} \quad k = 0, 1, \cdots, n \tag{39}$$

Using Eq. (38) and the definition of ω_{j0}, the first time derivative of ω_{j0} is

$$\dot{\omega}_{j0} = -\sum_{k=0}^{n}\rho_{jk}^{p}\mathbf{p}_{jk} - \sum_{k=0}^{n}\rho_{jk}^{d}\omega_{jk} \tag{40}$$

Applying Eq. (39) to Eq. (40) results in a system of n equations of the form,

$$\sum_{k=0}^{n}\rho_{jk}^{p}\mathbf{p}_{jk} = \mathbf{0} \tag{41}$$

The definition of $\bar{\mathbf{p}}_{jk}$ is used to rewrite Eq. (41) as

$$\mathbf{0} = \rho_{j0}^{p}\mathbf{p}_{j0} + \sum_{k=1}^{n}\rho_{jk}^{p}\mathrm{sgn}(q_{4,jk})[(-\mathbf{p}_{k0}^{\times} + p_{4,k0}\mathbf{1})\mathbf{p}_{j0} - q_{4,j0}\mathbf{q}_{k0}] \tag{42}$$

$$= \rho^p_{j0}\mathbf{q}_{j0} + \left[-\left(\sum_{k=1}^{n} \mathrm{sgn}(q_{4,jk})\rho^p_{jk}\mathbf{q}_{k0}\right)^{\times} + \sum_{k=1}^{n} \mathrm{sgn}(q_{4,jk})\rho^p_{jk}p_{4,k0}\mathbf{1}\right]\mathbf{p}_{j0} - p_{4,j0}\sum_{k=1}^{n} \mathrm{sgn}(q_{4,jk})\rho^p_{jk}\mathbf{p}_{k0} \tag{43}$$

which can be written as

$$-\mathbf{p}^{\times}_{j0}\sum_{k=1}^{n} \mathrm{sgn}(q_{4,jk})\rho^p_{jk}\mathbf{p}_{k0} = \left(\rho^p_{j0} + \sum_{k=1}^{n} \mathrm{sgn}(q_{4,jk})\rho^p_{jk}p_{4,k0}\right)\mathbf{p}_{j0} - p_{4,j0}\sum_{k=1}^{n} \mathrm{sgn}(q_{4,jk})\rho^p_{jk}\mathbf{p}_{k0} \tag{44}$$

The right-hand side of Eq. (44) is a linear combination of the vectors $\mathbf{p}_{j0}$ and $\sum_{k=1}^{n} \mathrm{sgn}(q_{4,jk})\rho^p_{jk}\mathbf{p}_{k0}$ and the left-hand side of the equation is the cross product of the same two vectors. The equality is only satisfied if

$$\mathbf{p}^{\times}_{j0}\sum_{k=1}^{n} \mathrm{sgn}(q_{4,jk})\rho^p_{jk}\mathbf{p}_{k0} = \mathbf{0} \tag{45}$$

Therefore, Eq. (44) simplifies to

$$\left(\rho^p_{j0} + \sum_{k=1}^{n} \mathrm{sgn}(q_{4,jk})\rho^p_{jk}p_{4,k0}\right)\mathbf{p}_{j0} - p_{4,j0}\sum_{k=1}^{n} \mathrm{sgn}(q_{4,jk})\rho^p_{jk}\mathbf{p}_{k0} = \mathbf{0} \tag{46}$$

The set of n equations that result represented in matrix form is

$$\mathbf{MP} = \mathbf{0} \tag{47}$$

The $3n \times 1$ column matrix $\mathbf{P}$ is defined

$$\mathbf{P} = \begin{bmatrix} \mathbf{p}^{\mathsf{T}}_{10} & \mathbf{p}^{\mathsf{T}}_{20} & \cdots & \mathbf{p}^{\mathsf{T}}_{n0} \end{bmatrix}^{\mathsf{T}} \tag{48}$$

The $3n \times 3n$ matrix $\mathbf{M}$ is defined

$$\mathbf{M} = \begin{bmatrix} m_{11}\mathbf{1} & m_{12}\mathbf{1} & \cdots & m_{1n}\mathbf{1} \\ m_{21}\mathbf{1} & \ddots & \cdots & \vdots \\ \vdots & \cdots & \ddots & m_{n-1|n}\mathbf{1} \\ m_{n1}\mathbf{1} & \cdots & m_{n|n-1}\mathbf{1} & m_{nn}\mathbf{1} \end{bmatrix} \tag{49}$$

where m_{jk} is defined

$$m_{jk} = \begin{cases} -\mathrm{sgn}(q_{4,jk})p_{4,j0}\rho^p_{jk} & \text{if } j \neq k \\ \rho^p_{j0} + \sum_{k=1}^{n} \mathrm{sgn}(q_{4,jk})\rho^p_{jk}p_{4,k0} & \text{if } j = k \end{cases} \tag{50}$$

The equation is satisfied if $\mathbf{P}$ is in the null space of $\mathbf{M}$; however, the formation has converged only if

$$\mathbf{P} = \mathbf{0} \tag{51}$$

Therefore, $\mathbf{M}$ fully spanning the vector space is a necessary and sufficient condition to guarantee convergence. The $\mathbf{M}$ matrix is strictly diagonally dominant if

$$\| m_{jj} \| > \sum_{k=1,k\neq j}^{n} \| m_{jk} \| \tag{52}$$

The left-hand side of the inequality is

$$\| m_{jj} \| = \left\| \rho^p_{j0} + \sum_{k=1}^{n} \mathrm{sgn}(q_{4,jk})\rho^p_{jk}p_{4,k0} \right\| = \rho^p_{j0} + \sum_{k=1}^{n} \mathrm{sgn}(q_{4,jk})\rho^p_{jk}p_{4,k0} \tag{53}$$

$$= \rho^p_{j0} + \sum_{k=1}^{n} sgn(q_{4,jk})\rho^p_{jk}p_{4,k0} \tag{54}$$

and the right-hand side of the inequality is

$$\sum_{k=1,k\neq j}^{n} \| m_{jk} \| = \sum_{k=1,k\neq j}^{n} \| -\mathrm{sgn}(q_{4,jk})p_{4,j0}\rho^p_{jk} \| = \sum_{k=1}^{n} p_{4,j0}\rho^p_{jk} \tag{55}$$

Plugging these quantities into Eq. (52) results in

$$\rho^p_{j0} + \sum_{k=1}^{n} \mathrm{sgn}(q_{4,jk})\rho^p_{jk}p_{4,k0} > \sum_{k=1}^{n} p_{4,j0}\rho^p_{jk} \tag{56}$$

Solving for ρ^p_{j0}

$$\rho^p_{j0} > \sum_{k=1}^{n} p_{4,j0}\rho^p_{jk} - \sum_{k=1}^{n} \mathrm{sgn}(q_{4,jk})\rho^p_{jk}p_{4,k0} \tag{57}$$

$$> \sum_{k=1}^{n} (p_{4,j0} - \mathrm{sgn}(q_{4,jk})p_{4,k0})\rho^p_{jk} \tag{58}$$

The quantity $[p_{4,j0} - \mathrm{sgn}(q_{4,jk})p_{4,k0}]$ satisfies the following inequality,

$$-1 \leq [p_{4,j0} - \mathrm{sgn}(q_{4,jk})p_{4,k0}] \leq 2 \tag{59}$$

therefore,

$$\sum_{k=1}^{n} [p_{4,j0} - \mathrm{sgn}(q_{4,jk})p_{4,k0}]\rho^p_{jk} \leq 2\sum_{k=1}^{n} \rho^p_{jk} \tag{60}$$

Thus, if

$$\rho^p_{j0} > 2\sum_{k=1}^{n} \rho^p_{jk} \tag{61}$$

the matrix $\mathbf{M}$ is strictly diagonally dominant, and fully spans the vector space [21]. Therefore, the only valid stable equilibrium condition of the spacecraft formation is Eq. (51). The class of decentralized attitude control laws thereby guarantees that the spacecraft within the formation will converge to the desired attitude trajectory.

Coordination Architectures

Equation (19) represents a class of decentralized control laws that differ by the coordination architecture used by the spacecraft formation. The choice of the formation-keeping behavior weights, ρ^p_{jk} and ρ^d_{jk}, determine the coordination architecture used. A nonzero ρ^p_{jk} and/or ρ^d_{jk} is referred to as a connection between spacecraft. The magnitude of ρ^p_{jk} and/or ρ^d_{jk} is referred to as the strength of the connection. Variants of coordination architectures can be created by altering the number of connections between spacecraft and the strength of the connections.

Four different coordination architectures for a six-spacecraft formation are presented in Fig. 1. The circles represent the individual spacecraft. Connections between the spacecraft are denoted by bidirectional arrows. The coordination architectures in Fig. 1 differ in the number of connections per spacecraft, c, used. Diagram B shows a coordination architecture with two connections per spacecraft. This type of coordination architecture is used by the velocity feedback controller presented in Lawton and Beard [17] and the "coupled-dynamics controller" presented in Lawton et al. [14]. The authors term the two-connection architecture the "ring" coordination architecture.

One interesting coordination architecture groups spacecraft in a formation into clusters of strongly connected spacecraft. The clusters

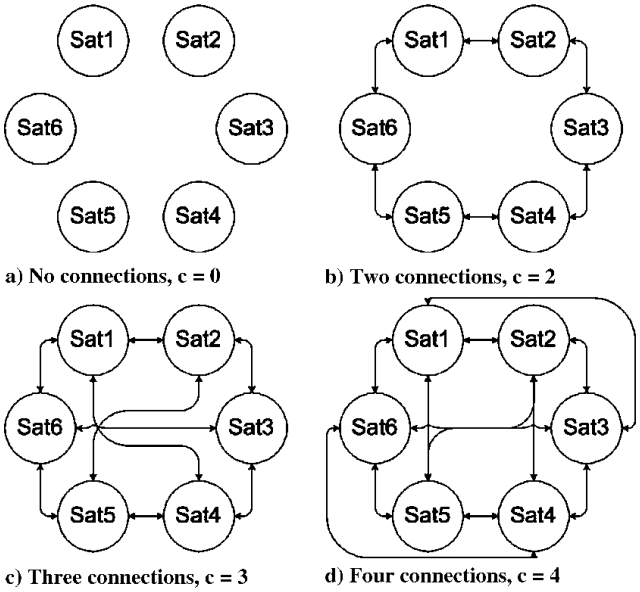

Fig. 1 Four decentralized coordination architectures using a different number of connections per spacecraft.

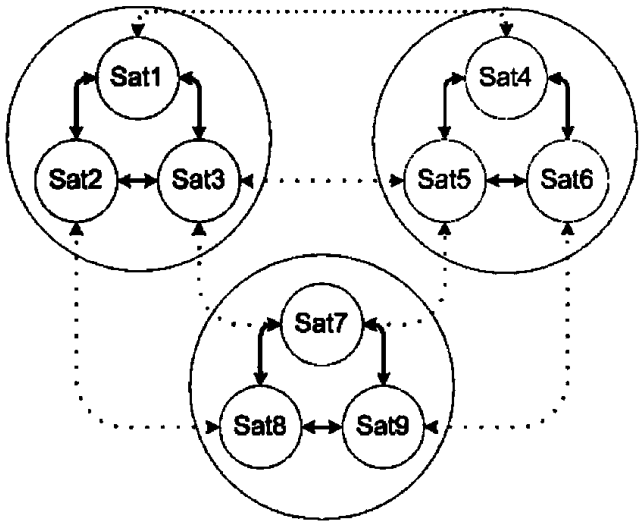

Fig. 2 A decentralized coordination architecture that groups spacecraft into clusters.

are then lightly connected through connections between spacecraft in different clusters. Figure 2 shows a nine-spacecraft coordination architecture that makes use of clusters. The nine spacecraft are grouped into three clusters of three spacecraft each. The strong connections within the clusters are represented by the solid bidirectional arrows. The weak connections between spacecraft in different clusters are denoted by the dotted bidirectional arrows.

Simulation Results

The performance and stability characteristics of the class of decentralized attitude control laws are investigated through numeric simulation. The analysis presented in the preceding section is reinforced using simulations of a four-spacecraft formation with no disturbance torques. A brief performance analysis of different coordination architectures is performed using simulations including constant disturbance torques.

The spacecraft are modeled as rigid bodies whose inertia matrices are defined

$$\mathbf{I}_j = \begin{bmatrix} 45.2156 & -1.1520 & -2.7811 \\ -1.1520 & 47.9560 & 1.3586 \\ -2.7811 & 1.3586 & 50.6733 \end{bmatrix} \text{kg} \cdot \text{m}^2 \quad \text{for } j = 1, 2, 3, 4 \tag{62}$$

The station-keeping behavior weights used in all of the simulations are

$$\begin{matrix} \rho^p_{j0} = 50 \\ \rho^d_{j0} = 70 \end{matrix} \quad \text{for } j = 1, 2, 3, 4 \tag{63}$$

The simulations require the definition of the desired attitude trajectory, $\mathcal{F}_0$, and the desired constant attitude offset from $\mathcal{F}_0$. The spacecraft formation is commanded to perform a 90 deg slew maneuver about the

$$\begin{bmatrix} 1 & 0 & 0 \end{bmatrix}^\mathsf{T}$$

axis expressed in $\mathcal{F}_0$. The slew is completed in 90 s. The spacecraft are commanded to be aligned with $\mathcal{F}_0$ with no attitude offset.

The performance of the spacecraft formation is measured using a station-keeping and a formation-keeping attitude error metric. The station-keeping attitude error metric is defined

$$\alpha(\bar{\mathbf{p}}_{10}, \bar{\mathbf{p}}_{20}, \cdots, \bar{\mathbf{p}}_{n0}) = \sqrt{\sum_{j=1}^{n} \|\Phi(\bar{\mathbf{p}}_{j0})\|^2} \tag{64}$$

where the function $\Phi(\bar{\mathbf{p}})$ calculates the Euler angle of the canonical quaternion. The formation-keeping attitude error metric is defined

$$\beta(\bar{\mathbf{p}}_{10}, \bar{\mathbf{p}}_{20}, \cdots, \bar{\mathbf{p}}_{n0}) = \sqrt{\sum_{j=1}^{n-1} \sum_{k=j+1}^{n} \|\Phi(\bar{\mathbf{p}}_{jk})\|^2} \tag{65}$$

A metric to measure the overall control effort exerted by the spacecraft in the formation is defined

$$\gamma(\mathbf{g}_1, \mathbf{g}_2, \cdots, \mathbf{g}_n) = \sqrt{\sum_{j=1}^{n} \|\mathbf{g}_j\|^2} \tag{66}$$

Numeric Validation of the Analytic Analysis

The first simulation presented is used to validate the stability and convergence analysis presented in the preceding section. A four-spacecraft formation is simulated with no disturbance torques. The formation-keeping behavior weights used in the simulation are defined

$$\begin{matrix} \rho^p_{jk} = 8 \\ \rho^d_{jk} = 15 \end{matrix} \quad \text{for } j, k = 1, 2, 3, 4 \quad \text{and} \quad j \neq k \tag{67}$$

which satisfy Eqs. (20) and (21), and therefore guarantee global asymptotic stability and convergence of the spacecraft formation's attitude.

Figure 3 contains three plots showing the results of the simulation. The station-keeping attitude error metric throughout the simulation is shown in the top plot. The middle plot shows the formation-keeping attitude error metric. The control effort metric is shown in the bottom plot.

The simulation results validate the stability and convergence analysis in the preceding section. The plots in Fig. 3 show that the spacecraft formation converges to the reference attitude trajectory. The station-keeping and formation-keeping attitude error metrics fall to the integration tolerance in approximately 40 s. At approximately 90 s, the value of the control effort metric falls to approximately zero, which represents the completion of the slew maneuver.

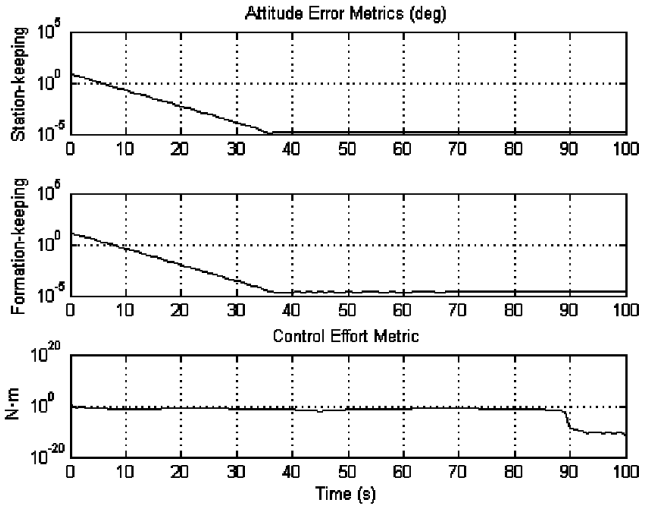

Fig. 3 The simulation results of a four-spacecraft formation with no unmodeled effects.

A Brief Performance Analysis of Different Coordination Architectures

Investigating the performance of different coordination architectures requires that some simulation parameters be held constant so that meaningful comparisons can be made. The spacecraft in the formation are initialized to the same attitude states in all of the simulations. A constant disturbance torque is included in the simulations to analyze the relative performance of the coordination architectures. The magnitude of the torque, 0.01 N · m, was chosen to create steady-state angular errors that are large enough to allow for performance comparisons. The axes defining the directions of the torques were generated randomly, so that each spacecraft would have a different tracking error. The analysis is simplified by maintaining a constant ratio for the proportional and derivative formation-keeping behavior weights for each connection in the coordination architectures. The derivative behavior weight is defined

$$\rho_{jk}^{d} = \frac{15}{8}\rho_{jk}^{p} \quad \text{for } j,k = 1,2,3,4 \quad \text{and} \quad j \neq k \tag{68}$$

Behavior Weight Variation

Five simulations of a four-spacecraft formation are performed. Each simulation uses a three-connection per spacecraft coordination architecture. All of the connections are equally weighted. The simulations differ by the magnitude of the formation-keeping behavior weights used.

The formation-keeping behavior weights used in each simulation are summarized in Table 2. These values satisfy Eqs. (20) and (21), and therefore guarantee global asymptotic stability and convergence of the attitude of spacecraft within the formation. The steady-state values of the attitude error metrics found in the simulations are summarized in Table 2. The steady-state values of both the station-keeping and formation-keeping attitude error metrics decrease with increasing connection strength. Figure 4 contains plots of the control effort metric during each of the simulations. Only one curve is visible because the control effort metric values throughout the five simulations are nearly identical, except for some slight differences at the beginning of the maneuver. The steady-state value of the control effort metric for all of the simulations is approximately 0.02 N · m.

Variation of the Number of Connections Per Spacecraft

The effect of varying the number of connections per spacecraft in a coordination architecture is investigated using four simulations of a four-spacecraft formation. Four simulations are performed using coordination architectures with 0, 1, 2, and 3 connections per spacecraft. The connections between spacecraft used in each of the simulations are summarized in Table 3. The formation-keeping behavior weights for each connection are held constant over the

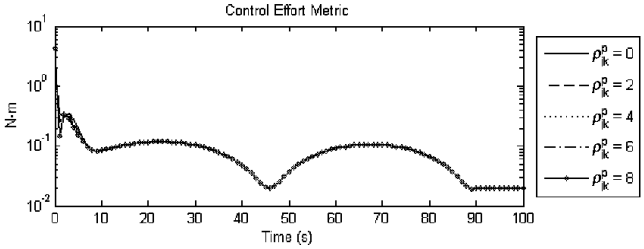

Fig. 4 Control effort metric using different magnitudes for the formation-keeping behavior weights.

formation and are defined

$$\rho_{jk}^{p} = 8 \tag{69}$$

$$\rho_{jk}^{d} = 15 \tag{70}$$

The steady-state values of the attitude error metrics for each simulation are summarized in Table 4. The table shows the decrease in the steady-state values of the attitude error metrics with an increasing number of connections per spacecraft. Figure 5 contains plots of the control effort metric during each of the simulations. As in the preceding set of simulations, only one curve is visible because the control effort metric values throughout the five simulations are nearly identical, except for some slight differences at the beginning of the maneuver. The steady-state value of the control effort metric for all of the simulations is approximately 0.02 N · m.

Discussion of Simulation Results

The results of the simulations demonstrate that an improvement in the steady-state values of the attitude error metrics can be achieved

Table 2 The formation-keeping behavior weights and steady-state attitude error metric values for the five simulations

Proportional behavior weight (ρ_{jk}^{p})	Derivative behavior weight (ρ_{jk}^{d})	Station-keeping error metric (α), deg	Formation-keeping error metric (β), deg
0.00	0.00	8.00×10^{-4}	1.18×10^{-3}
2.00	3.75	7.42×10^{-4}	1.02×10^{-3}
4.00	7.50	7.01×10^{-4}	8.96×10^{-4}
6.00	11.25	6.71×10^{-4}	7.99×10^{-4}
8.00	15.00	6.48×10^{-4}	7.21×10^{-4}

Table 3 The connections between spacecraft used in the four simulations

Number of connections per spacecraft (c)	Connections between the jth and kth spacecraft (j,k)
0	none
1	(1,4), (2,3)
2	(1,3), (1,4), (2,3), (2,4)
3	(1,2), (1,3), (1,4), (2,3), (2,4) ,(3,4)

Table 4 The steady-state attitude error metric values for the four simulations

Number of connections per spacecraft (c)	Station-keeping error metric (α), deg	Formation-keeping error metric (β), deg
0	8.00×10^{-4}	1.18×10^{-3}
1	7.37×10^{-4}	1.01×10^{-3}
2	6.78×10^{-4}	8.23×10^{-4}
3	6.48×10^{-4}	7.21×10^{-4}

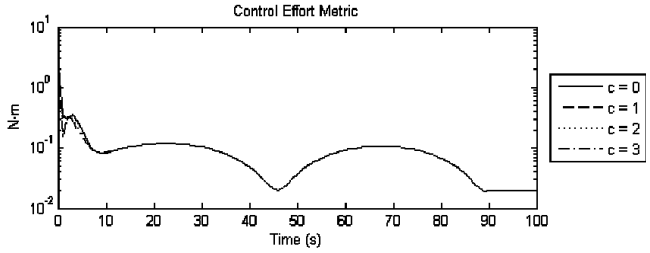

Fig. 5 Control effort metric using a different number of connections per spacecraft.

by increasing either the strength of the connections or the number of connections per spacecraft of the coordination architecture.

The decrease in the steady-state value of the formation-keeping attitude error metric shown in the simulations is intuitive. Increasing the number of connections per spacecraft leads to a better estimate of the "average" attitude of the formation. The improved estimate allows for more accurate control. Increasing the strength of the connections elevates the importance of the formation-keeping behavior, resulting in greater control effort being expended to satisfy the formation-keeping behavior.

The improvement in the steady-state value of the station-keeping attitude error metric is not as intuitive, and an examination of the calculation of the station-keeping attitude error metric at steady state is required. For small angular errors, like those realized in the steady-state condition, the function Φ can be approximated as

$$\Phi(\bar{\mathbf{p}}) \approx 2 \parallel \mathbf{p} \parallel \tag{71}$$

The resulting approximation of the station-keeping attitude error metric is

$$\alpha \approx 2 \sqrt{\sum_{j=1}^{n} \|\mathbf{p}_{j0}\|^2} \tag{72}$$

The approximate α is the root-sum-square (RSS) of the distances of the points defined by the $\mathbf{p}_{j0}$ from the origin. Applying the small angle approximation to the formation-keeping attitude error metric results in

$$\beta = 2 \sqrt{\sum_{j=1}^{n-1} \sum_{k=j+1}^{n} \|\mathbf{p}_{j0} - \mathbf{p}_{k0}\|^2} \tag{73}$$

The approximate β is the RSS of the distances of the points defined by the $\mathbf{p}_{j0}$ from one another, and is a measure of the spread of those points.

The constant disturbance torques used in the simulations were generated so that they are equal in magnitude and have a random direction. For the "$c = 0$" and the "$\rho^p_{jk} = \rho^d_{jk} = 0$" simulation,[††] the steady-state $\mathbf{p}_{j0}$ can be calculated using

$$\mathbf{p}_{j0} = -\frac{1}{\rho_{j0}} \mathbf{g}_{d_j} \tag{74}$$

Because the magnitude of the constant disturbance torque and the proportional station-keeping behavior weight are constant over the formation, the points defined by the steady-state $\mathbf{p}_{j0}$ lie on the surface of a sphere with a radius $\parallel \mathbf{g}_{d_j} \parallel / \rho_{j0}$ that is centered at the origin. The randomly-generated directions of the constant disturbance torques results in a random distribution of the $\mathbf{p}_{j0}$ points over the surface of that sphere.

The simulations performed using coordination architectures with $c > 0$ and $\rho^p_{jk}, \rho^d_{jk} > 0$ resulted in lower steady-state values of β. Equation (73) requires a decrease in the spread of the $\mathbf{p}_{j0}$ points for a decrease in the value of β. If the $\mathbf{p}_{j0}$ points are evenly, or nearly evenly, distributed on the surface of the sphere, as is the case in the simulations that have been presented, a decrease in the spread results in the points moving toward the origin. Equation (72) requires a decrease in the value of α for a decrease in the distances of the $\mathbf{p}_{j0}$ points from the origin. Therefore, the decrease in the steady-state value of α is expected for simulations using coordination architectures with a greater number of connections or stronger connections between spacecraft.

The results of the simulations also show that the decrease in the steady-state value of the attitude error metrics is achieved without increasing the steady-state value of the control effort metric. The spacecraft in the simulations reach a steady-state once the control torques applied by the spacecraft, $\mathbf{g}_j$, reach a constant value that is equal in magnitude and opposite in direction to the constant disturbance torque, $\mathbf{g}_{d_j}$, applied to the spacecraft.

$$\mathbf{g}_j = -\mathbf{g}_{d_j} \quad \forall\ j \tag{75}$$

Therefore, the steady-state value of the control effort metric is dependent solely on the magnitude of the constant disturbance torques used in the simulations. The expected steady-state value of the control effort metric for the simulations is

$$\gamma = \sqrt{\sum_{j=1}^{n} \|\mathbf{g}_{d_j}\|^2} = \sqrt{0.01^2 + 0.01^2 + 0.01^2 + 0.01^2}\ \mathrm{N \cdot m}$$
$$= 0.02\ \mathrm{N \cdot m} \tag{76}$$

which is equal to the value found in the simulations.

Summary and Conclusions

The primary contribution of this work is the development and analysis of a class of decentralized coordinated attitude tracking control laws that guarantee global asymptotic stability and convergence of the attitude of spacecraft within a formation. Emphasis is placed on the use of physically significant relative attitude variables and providing a global asymptotic stability and convergence proof for the class of decentralized attitude control laws. A corollary of Barbalat's Lemma is used to prove that the class of decentralized attitude control laws guarantees the global asymptotic stability of the attitude of spacecraft within a formation, and convergence is shown to be a consequence of the closed-loop equations of motion. The results of a numeric simulation of a four-spacecraft formation performing a slew maneuver reinforced the analytic results.

The class of decentralized attitude control laws consists of control laws that use different coordination architectures. Coordination architectures can vary by the number and strength of the connections between spacecraft. The performance effects of varying the number and strength of the connections are briefly investigated using numeric simulations of a spacecraft formation with constant disturbance torques. The simulation results show that increasing either the number or strength of the connections decrease the steady-state values of both the station-keeping and formation-keeping attitude error metrics. Simulation results and analytic analysis show that the steady-state value of the control effort metric is independent of coordination architecture.

References

[1] Davison, E., "The Decentralized Stabilization and Control of a Class of Unknown Non-Linear Time-Varying Systems," *Automatica: The Journal of IFAC, the International Federation of Automatic Control*, Vol. 10, No. 3, May 1974, pp. 309–316.

[2] Aoki, M., and Li, M. T., "Partial Reconstruction of State Vectors in Decentralized Dynamic Systems," *IEEE Transactions on Automatic Control*, Vol. 18, No. 3, 1973, pp. 289–292.

[3] Balch, T., and Arkin, R. C., "Behavior-Based Formation Control for Multirobot Teams," *IEEE Transactions on Robotics and Automation*, Vol. 14, No. 6, 1998, pp. 926–939.

[4] Beard, R., Lawton, J., and Hadaegh, F., "A Coordination Architecture

[††]The "$c = 0$" and the "$\rho^p_{jk} = \rho^d_{jk} = 0$" simulation use the same coordination architecture and therefore have identical results.

for Spacecraft Formation Control," *IEEE Transactions on Control Systems Technology*, Vol. 9, No. 6, 2001, pp. 777–790.

[5] Wang, P., and Hadaegh, F., "Coordination and control of multiple microspacecraft moving in formation," *Journal of the Astronautical Sciences*, Vol. 44, No. 3, 1996, pp. 315–355.

[6] Wang, P., Hadaegh, F., and Lau, K., "Synchronized Formation Rotation and Attitude Control of Multiple Free-Flying Spacecraft," *Journal of Guidance, Control, and Dynamics*, Vol. 22, No. 1, 1999, pp. 28–35.

[7] Wang, P., Yeh, J., and Hadaegh, F., "Synchronized Rotation of Multiple Autonomous Spacecraft with Rule-Based Controls: Experimental Study," *Journal of Guidance, Control, and Dynamics*, Vol. 24, No. 2, 2001, pp. 352–359.

[8] Kang, W., Sparks, A., and Banda, S., "Coordinated Control of Multisatellite Systems," *Journal of Guidance, Control, and Dynamics*, Vol. 24, No. 2, 2001, pp. 360–368.

[9] Kang, W., and Yeh, H.-H., "Co-ordinated Attitude Control of Multi-Satellite Systems," *International Journal of Robust and Nonlinear Control*, Vol. 12, No. 2–3, 2002, pp. 185–205.

[10] Kang, W., Xi, N., and Sparks, A., "Theory and Applications of Formation Control in a Perceptive Referenced Frame," *Proceedings of the IEEE Conference on Decision and Control*, Vol. 1, IEEE, Piscataway, NJ, 2000, pp. 352–357.

[11] Kang, W., Yeh, H.-H., and Sparks, A., "Coordinated Control of Relative Attitude for Satellite Formation," AIAA Paper 2001-4093, Aug. 2001.

[12] Kang, W., and Sparks, A., "Coordinated Attitude and Formation Control of Multi-Satellite Systems," AIAA Paper 2002-4655, Aug. 2002.

[13] Ren, W., and Beard, R. W., "Virtual Structure Based Spacecraft Formation Control with Formation Feedback," AIAA Paper 2002-4963, Aug. 2002.

[14] Lawton, J., Beard, R. W., and Hadaegh, F. Y., "Elementary Attitude Formation Maneuvers Via Leader-Following and Behavior-Based Control," AIAA Paper 2000-4442, Aug. 2000.

[15] Beard, R. W., Lawton, J., and Hadaegh, F. Y., "A Feedback Architecture for Formation Control," *American Control Conference*, Vol. 3, American Automatic Control Council, Evanston, IL, 2000, pp. 3975–3979.

[16] Lawton, J., Young, B., and Beard, R., "A Decentralized Approach to Elementary Formation Maneuvers," *Proceedings of The IEEE International Conference on Robotics and Automation*, Vol. 3, IEEE, Piscataway, NJ, 2000, pp. 2728–2733.

[17] Lawton, J. R., and Beard, R. W., "Synchronized Multiple Spacecraft Rotations," *Automatica: The Journal of IFAC, the International Federation of Automatic Control*, Vol. 38, No. 8, 2002, pp. 1359–1364.

[18] Hall, C. D., Tsiotras, P., and Shen, H., "Tracking Rigid Body Motion Using Thrusters and Momentum Wheels," *Journal of the Astronautical Sciences*, Vol. 50, No. 3, 2002, pp. 311–323.

[19] Bhat, S. P., and Bernstein, D. S., "A Topological Obstruction to Global Asymptotic Stabilization of Rotation Motion and the Unwinding Phenomenon," *Proceedings Of American Control Conference*, Vol. 5, American Automatic Control Council, Evanston, IL, 1998, pp. 2785–2789.

[20] Slotine, J. E., and Li, W., *Applied Nonlinear Control*, Prentice–Hall, Upper Saddle River, NJ, 1991.

[21] Burden, R. L., and Faires, J. D., *Numerical Analysis*, 7th ed., Brooks/Cole, Pacific Grove, CA, 2001.